UNIVERSITY OF CALIFORNIA SAN DIEGO

The Role of Neuromodulators in Learning

A Thesis submitted in partial satisfaction of the requirements for the degree
Master of Science

in

Biology

by

Sara Sadat Emami

Committee in charge:

Professor Takaki Komiyama, Chair
Professor Robert Malinow, Co-Chair
Professor James Kadonaga

2018

The Thesis of Sara Sadat Emami is approved, and it is acceptable in quality and form for publication on microfilm and electronically:

_____

_____
Co-Chair

_____
Chair

University of California San Diego

2018

TABLE OF CONTENTS

LIST OF FIGURES

ACKNOWLEDGEMENTS

I would like to thank the Komiyama Lab for allowing me to grow as a student and researcher. Throughout my time in the lab, I met a few individuals who had an influential impact on me and my work.

Firstly, I would like to thank Dr. Nathan Hedrick for taking me under his wing and constantly teaching, encouraging, and supporting me through all my endeavors, not just research. He has been the most amazing mentor and I have been lucky to work with him. Not only do I learn from him, but he challenges me to think in different perspectives. He has helped me grow tremendously as a person and I believe all the skills I have learned from him will benefit my future in medicine.

Secondly, I would like to thank Dr. Takaki Komiyama, my advisor and committee chair, for also being an amazing mentor and giving me the opportunity to pursue my master's thesis at the lab. Despite his busy schedule, he continued to share with me his knowledge, time, and patience. In addition, he has helped me gain a much deeper understanding and appreciation for science.

Thirdly, I would like to thank the rest of the lab members for not only teaching me and creating an environment where I can grow, but serving as like a second family. I have been incredibly grateful to have met all these individuals.

Also, I would like to thank Dr. Roberto Malinow and Dr. James Kadonaga for being a part of my master's thesis committee and for their support throughout the process.

I would like to thank my parents who have been my constant support system and have helped me get through it all. They helped me get through all my obstacles like tireless nights at the lab, making sure I got home safely from bizarre times at the lab, and for even celebrating my smallest achievements.

I would also like to thank my sister, Sophy, who inspired me to get into neuroscience research. Engaging in this type of research has made me interested in continuing this in medical school in hope to one day help individuals suffering like my sister.

Lastly, I would like to thank all the mice who have sacrificed their lives for science. Much of our advancements in research would not have been possible without animal research.

ABSTRACT OF THE THESIS

The Role of Neuromodulators in Learning

by

Sara Sadat Emami

Master of Science in Biology

University of California San Diego, 2018

Professor Takaki Komiyama, Chair
Professor Roberto Malinow, Co-Chair

Neuromodulators have been associated with learning but much of our knowledge comes from pharmacological and *in vitro* studies. Therefore, a mechanistic understanding of how these neuromodulators play a role on learning *in vivo* is lacking. We used motor learning as a robust learning platform previously established by our lab since the resulting structural and phenotypic changes are known in detail. Using this platform, we studied neuromodulators in high degrees of specificity in learning animals using both a loss and gain of function approach. Our loss of function approach consisted of a series of surgeries, viral injections, and CRISPR. However, with cutting-

edge technology, came obstacles. Therefore, the loss of function approach served as a technical side of the project.

In contrast, the gain of function was the experimental side of the project. Our investigation began with neuromodulator acetylcholine, but hope to continue with all the neuromodulators. By using the tools of optogenetics, the acetylcholine system was upregulated in the motor cortex and the resulting behavioral effects were analyzed in mice learning a lever-press task. Since acetylcholine is involved in attention, I hypothesized that excess acetylcholine in the mouse motor cortex would accelerate motor learning. If my hypothesis is correct, then we can investigate exactly how acetylcholine controls plasticity during learning using *in vivo* two-photon calcium imaging. Successfully using various cutting-edge techniques and gaining a mechanistic understanding of how neuromodulators affect learning will expand our understanding of the brain and contribute to public health as better pharmacological approaches can be created to target these systems.

Introduction

Neuromodulators are chemical signals that shape – as opposed to drive – neural activity in a context-dependent manner. Learning requires activity-dependent changes to neurons. Therefore, neuromodulatory regulation of neuronal activity states could contribute to learning. Indeed, previous studies have shown that various neuromodulators are associated with different behavioral states that contribute to learning. For example, reward prediction, arousal, and attention have been associated with neuromodulators dopamine, norepinephrine, and acetylcholine, respectively[1-4].

In the case of dopamine, both the ablation of dopamine-releasing (or "dopaminergic") neurons and the specific pharmacological blockade of dopamine receptors in the rat motor cortex has been shown to impair motor skill learning[5]. The learning impairment suggests that dopamine in the motor cortex is necessary for normal acquisition of motor skill learning. Similarly, selective lesions of acetylcholine-releasing (or "cholinergic") neurons in the rat motor cortex significantly impaired motor learning[6]. Consistent with their role in learning, neuromodulators modulate how the brain rewires itself through plasticity. Lesions of cholinergic inputs to the rat motor cortex blocked the normal expansion of the cortical forelimb representation during training of a reach task, influencing a large-scale circuit plasticity associated with learning[6]. Furthermore, blockade of dopamine receptors, DA1 or DA2, with respective antagonists in the rat motor cortex resulted in a decreased expression of long-term potentiation, a type of synaptic plasticity associated with learning. These findings suggest that dopamine in the motor cortex is necessary for synaptic plasticity[5]. Likewise, literature has supported noradrenergic control over synaptic plasticity as well[7-8]. All these findings and many

more support the association of neuromodulators with learning on three different levels: phenotypic behavior, large-scale circuit plasticity, and synaptic plasticity[9-10]. However, much of our knowledge on this association comes from pharmacological and *in vitro* slice studies which lack specificity and are under non-physiological conditions. Thus, a mechanistic understanding of the role of neuromodulators on learning is largely lacking.

To address this, we used a combination of cutting-edge approaches to thoroughly investigate the function of neuromodulators with high degrees of specificity in learning animals. Namely, we combined multiple genetic manipulations with 2-photon imaging in an established learning framework, giving us unprecedented control over the neuromodulatory systems. Eventually, we will study every neuromodulator's role on learning. However, a learning platform for studying these neuromodulators needs to be established first. Thus, our experiments were carried out for a subset of neuromodulators (acetylcholine, dopamine, and norepinephrine) before the project is extended to all other neuromodulators.

Fortunately, our lab has established both a robust learning platform in which we can monitor the development of a stereotype movement pattern, and we have also identified cellular correlate of this learning, in the form of somatostatin-expressing inhibitory interneuron (SOM) and pyramidal neuron plasticity[11]. Specifically, simultaneous structural changes were seen on SOM cells and excitatory pyramidal cells in layer 2/3 of the mouse motor cortex over two weeks of learning. The motor learning paradigm involved a simple lever-press task while both changes in behavior and structural plasticity of the aforementioned cells were analyzed throughout learning[11-12]. Furthermore, layer 2/3 of the primary motor cortex (M1) is where motor information is

processed and the plasticity observed is critical for motor learning. Since neuromodulators play an essential role in learning, it is highly likely that they exert their modulatory effects on these two identified critical loci of motor plasticity. Thus, we used motor learning as a robust platform to study the role of neuromodulators on learning-related plasticity. Not only is this platform to our advantage in terms of knowing the specific cellular phenotypes associated with motor learning, but also because our lab has already developed the expertise on this learning paradigm. Furthermore, specific neuromodulators are already found to have an important role on motor learning[6-7]. Thus, we can investigate how the plasticity of the two cell types in the motor cortex and the behavioral phenotype deviate from normal conditions when the neuromodulatory systems are perturbed.

Therefore, by using motor learning as our learning platform, we investigated the mouse motor cortex to gain insight on the mechanistic role of neuromodulators. To elucidate a complete mechanistic understanding, we performed both loss-of-function and gain-of-function experiments. For the loss-of-function experiments, specific neuromodulatory receptors were knocked out from a sparse population of layer 2/3 cells in the mouse motor cortex using a CRISPR-based genome editing approach[13]. Cre-dependent mammalian expression vectors were designed by Dr. Nathan Hedrick, a post-doctoral fellow in the lab and leading scientist of the project, containing small guide RNAs (sgRNA) targeting specific neuromodulatory receptors for knock-out, Cas 9 endonuclease enzyme guided by the sgRNAs to cut specific sites of DNA, and green fluorescent protein (GFP) as the reporter gene. Once the CRISPR-based knock out of the targeted genes was verified by RNAscope (an advance RNA *in situ* hybridization

technique), the constructs were introduced into excitatory pyramidal cells in layer 2/3 of the motor cortex of timed embryonic mouse brains via *in utero* electroporation (IUE). Once the mice were born and matured, viral-mediated Cre-recombinase was introduced to a sparse population of M1 layer 2/3 cells and a glass window was implanted over M1. Initially, the Cas9 and GFP genes were in the antisense direction preventing their transcription. Once Cre was introduced to cells containing the engineered DNA, however, the gene was inverted into the sense direction, initiating Cas9-GFP gene expression. The expression of Cas9 protein led to the knock out of the specific neuromodulatory receptors. By using two-photon imaging of the fluorescently labeled cells, the structural plasticity of these neurons was then investigated in vivo of learning and behaving mice to see how receptor knock-out affected learning[14].

For our gain-of-function experiments, an optogenetic approach was utilized because it allows for optical, *in vivo* control of specific neuronal populations. This mechanism of activating neurons can elicit complex behaviors. For example, optogenetic activation of artificially expressed channelrhodopsin-2 (ChR2), a blue light-gated cation channel, in the neurons within the ventromedial hypothalamus in male mice induced aggressive attacks immediately from the onset of light stimulation to its termination towards male and female mice as well as inanimate objects[15]. For our project, we wanted to perform a similar experiment with neuromodulators that can potentially artificially impose a cognitive or behavioral state in each animal; for example, if excess cortical acetylcholine led to more attentive mice. Thus, optogenetic activation of specific cells could elicit such potential subtle behaviors, since there's evidence of eliciting extreme behaviors[15]. For this reason, targeted neuromodulatory systems in the

M1 were artificially upregulated via optogenetics in learning animals and the resulting effects on learning were analyzed.

Optogenetics allows for a high degree of spatial and temporal control over the release of neuromodulators during learning. We began this phase of our project by perturbing the acetylcholine system in the mouse brain since M1 is densely innervated with cholinergic fibers throughout all its layers[16]. The brain's cortex is most densely innervated by cholinergic fibers originating from the basal forebrain, particularly from the nucleus basalis in the substantia innominata[16]. Thus, the majority of cholinergic axons extend from their somata in the substantia innominata and terminate all over the cortex, thereby providing most of the acetylcholine released in the brain's cortex[17-18]. A choline acetyltransferase (ChAT) promoter-driven Cre mouse line was used in which Cre-recombinase was only present in cells that expressed ChAT, an enzyme required for the synthesis of acetylcholine. Then, either Cre-dependent ChR2-tdTomato or saline was injected blindly into the substantia innominata and a cranial window was implanted over the primary motor cortex to allow for illumination during learning. Thus, we selectively stimulated cholinergic fibers in M1 that contained the viral-mediated expression of ChR2 originating from the substantia innominata. Ultimately, we gained an optogenetic control of on the endogenous release of acetylcholine from these cholinergic neurons in the mouse M1 during learning. Thus, optogenetics can reveal during what phases of learning the neuromodulator is most effective as the upregulation of the neuromodulatory system effects on learning and plasticity are analyzed.

As noted, previous literature has shown neuromodulator acetylcholine associated with attention[19]. Lesioned cortical cholinergic inputs has led to attentional impairments in

rats[21] and administration of the acetylcholine agonist, nicotine, has shown an attentional improvement in mice[21]. Since acetylcholine is associated with attention and learning[6], we hypothesized that an excess of cortical acetylcholine in M1 would affect the early stages of learning and lead to an acceleration of learning the motor task. Since acetylcholine affects synaptic plasticity[9-10], we also hypothesized that excess cortical acetylcholine would enhance the formation of new synaptic contacts during learning. Since behavior is correlated to plasticity, we would use the behavioral results to guide the imaging experiments. Even though our two approaches are independent of each other, they complement each other such that our results from one phase can guide our experiments in the other. For example, if the upregulation of the acetylcholine system produced no change on learning, then we would no longer continue the loss-of-function experiments with this neuromodulator. However, if we observe as we hypothesized that release of excess acetylcholine in the motor cortex accelerates learning during the initial phases of learning, then we would investigate how the initial phases of learning are affected by specific acetylcholine receptor knock-outs. By investigating the resulting effects of these experimental manipulations on both phenotypic behavior and structural plasticity of cells in the motor cortex of awake, behaving mice throughout learning a motor task, we can finally elucidate the mechanism by which neuromodulators affect learning-related plasticity.

All in all, the long-term goal of this project is to better understand how neuromodulators affect learning. The more immediate goal was to focus on a subset of neuromodulators and gain a mechanistic understanding of their role in learning from loss-of-function and gain-of-function experiments.

Results:

Loss-of-Function.

For our loss-of-function experiments, we targeted the deletion of specific neuromodulatory receptors via CRISPR-based genome editing using a series of cutting-edge techniques (Figure 1). Firstly, the Cre-recombinase-dependent CRISPR constructs that included sequences targeting a specific class of neuromodulatory receptors were introduced into a vector with Cas9 and GFP sequences in the antisense orientation (Figure 1a). Since these genes were in the reversed orientation, they were inactive. Only once Cre-recombinase was introduced would these genes be activated and expressed.

Before introducing the CRISPR constructs *in vivo,* RNAscope was performed *in vitro* to visualize mRNA and validate the efficacy of the CRISPR constructs. RNAscope was performed by Dr. Miguel Tillo from the Bloodgood Lab. To test the efficacy of our M1 muscarinic acetylcholine receptor, RNAscope was performed for Cholinergic Receptor Muscarinic 1 (CHRM1) and enhanced green fluorescent protein (EGFP) on DIV3 hippocampal organotypic slices sparsely transfected with gold particles containing gCHRM1-Cas9-EGFP and Cre-recombinase. Transfected neurons that began to express EGFP, no longer expressed CHMR1 mRNA (Figure 2). By using RNAscope, we verified the CRISPR construct's ability to successfully knockdown targeted neuromodulatory receptor mRNA in a Cre-dependent manner within neurons.

The validation of our CRISPR constructs *in vitro* allowed the introduction of our verified CRISPR constructs *in vivo.* During *in utero* electroporation, the CRISPR construct specific to knockdown of a particular neuromodulatory receptor type and a

vector containing the mCherry reporter gene were both introduced into timed embryonic mice brains[22]. Immediately after birth, the electroporated pups were observed for mCherry expression over their right forelimb area in the brain, which is visible through the thin skin above a pup's skull. Then, successful delivery of the CRISPR construct via IUE into L2/3 excitatory cortical pyramidal cells was confirmed by mCherry-positive pups (Figure 3a).

Once the mCherry-positive pups matured and reached adulthood, a craniotomy was performed and diluted AAV-Cre viral injections were directed into the same region of M1 that displayed positive mCherry expression. The targeted injection of diluted AAV-Cre labeled a sparse population of L2/3 neurons. The presence of mCherry expression indicated successful delivery of the CRISPR constructs during IUE and verified the survival of these constructs through adulthood (Figure 3b).

Once AAV-Cre was introduced into the same L2/3 excitatory pyramidal cells in M1 that were mCherry positive, Cre oriented the Cas9-GFP gene within the CRISPR construct into the correct orientation by utilizing the loxP sites. Once in the correct orientation, Cas9-sgRNA-mediated genome editing was initiated and GFP was expressed. Ultimately, GFP-positive cells indicated successful Cre-lox system activity within the cells expressing the CRISPR construct.

After the series of surgeries, we ultimately searched for neurons with co-expression of green and red fluorescence indicating both successful Cre-dependent CRISPR construct delivery and Cre-lox activity leading to knockdown of the neuromodulatory receptor within the co-labeled neuron. Once adult mice recovered from surgery, they underwent two weeks of training of a lever-press task with

simultaneous two-photon calcium imaging. However, a problem was faced when we began imaging the co-expressed neuron's in alive and behaving animals.

Despite visualizing the presence of co-labeled neurons, the GFP expression of these neurons was too dim (Figure 4). Low GFP expression was observed during two photon calcium imaging hindering our ability to follow the structural plasticity of the neuron throughout learning. The lack of visibility of defined structural details of the neuron led us to further investigate for alternative methods to combat this challenge.

Gain-of-Function:

During the trouble-shooting period of our loss-of-function experiments, I began working on the gain-of-function experiments. In the gain-of-function experiments, we used light to control genetically modified cells *in vivo* by introducing ChR2. We began investigating the hyperactivation of the acetylcholine system. Before conducting the experiments, we had to confirm the accuracy of our methodological approaches. ChAT-Cre mice, mice with Cre activity in all their cholinergic neurons, were first injected with viral-mediated, Cre-dependent ChR2-enhanced yellow fluorescent protein (EYFP) into their substantia innominata. After adjustments to viral volume, coordinates, and injection speeds, the stereotaxic injections were modified accordingly. Images of coronal sections from the injected brain were compared to a reference image from the Allen Brain Atlas. Our results indicated dense expression of ChR2-EYFP in the substantia innominata region (Figure 5)[23]. In addition, ChAT-positive and ChR2-positive somata were present in the substantia innominata and all the ChR2-positive were co-labeled with ChAT (Figure 6a). Since these cholinergic neurons project to the motor cortex, the presence of labeled axons was also analyzed in M1. ChAT-positive and ChR2-positive axons were

confirmed in M1 (Figure 6b). This all indicated the successful targeting and introduction of viral ChR2 into cholinergic neurons.

After confirming the introduction of viral, Cre-dependent ChR2 into cholinergic neurons projecting to the motor cortex, the surgeries were continued and those mice were used for the behavioral experiments. However, since we hypothesized that the upregulation of the acetylcholine system may affect plasticity within the critical cellular loci in the motor cortex, we changed our virus to ChR2-tdTomato to allow for the potential of imaging GFP-expressing cortical cells as a next step. By changing to ChR2-tdTomato, our experiments are kept as consistent as possible, and cortical GFP injection will allow us to image these cells to visualize any structural changes resulting from our experimentation during learning.

Our experiments continued as Cre-dependent ChR2-tdTomato or saline was blindly injected into the substantia innominata of ChAT-Cre mice (Figure 7). Our control group had all the same parameters except that saline was injected rather than the virus. Tubes of ChR2-tdTomato or saline were prepared by N. Hedrick or other members in the lab and given to me with an assigned experiment number, such that all the experiments were conducted blindly and I had no internal bias influencing the outcome of the experiments. After mice underwent surgery, viral injection, behavioral training, and histology, their brain tissues were checked for labeled cell bodies in the SI. ChR2-tdTomato injections also showed overlapping ChAT-positive and ChR2-positive cells within the SI (Figure 8b) and some labeled in M1(Figure 9b).

We gained a confirmation of accurate targeting of our cells with the new virus. Next, water-restricted mice underwent behavioral training of the simple-lever press task

after 3-4 weeks post-injection. Based on previous literature, the time between injection and training is the amount of time needed for ChR2 expression in the mouse motor cortex to stabilize following viral injection of ChR2[24]. During behavioral training, ChR2-tdTomato and saline injected mice learned to press a lever while their behavioral outputs were recorded. For every mouse during each trial, the blue light was on during the entire cue period. During the cue period, the blue light illuminated over the cranial window to activate cholinergic fibers expressing ChR2 in the mouse motor cortex. The cue period started with an auditory cue and illumination of blue light, lasted for 10 seconds or until the mouse received a reward, then was followed by the intertrial interval (ITI). During the ITI, no light was on and the mouse was not rewarded or punished. The cue period followed afterwards again. A simplified image of this task schematic is presented in figure 10.

Results from behavioral training were observed. Different behavioral parameters were compared between ChR2-tdTomato-injected mice (n = 12) and saline-injected mice (n = 9). The percent rewarded of each session was compared between the two groups for each session across 14 days. ChR2-expressing mice showed an increase in reward rate within the early stages of learning when compared to the saline-injected mice (Figure 11). The cue to movement and cue to reward time were also compared between the two groups. Cue to movement is the time from the onset of the auditory cue to when the mouse physically touched the lever, regardless if they were successful. Cue to reward is the time from the onset of the auditory cue to when the mouse successfully pressed the lever beyond the threshold and received the water reward. Percent rewarded represents the percentage of trials in which the mouse pressed the

lever beyond a set threshold and received a water reward. ChR2-expressing mice were reacting faster during the early stages of learning (Figure 11). From comparison between groups, these results were consistent with previous findings from our lab indicating that the mice from both groups were learning the lever-press task[10].

Next the correlation of rewarded trials between both groups were compared and analyzed. The correlation of rewarded trials of control mice showed a general increase within sessions (Pearson's correlation, p-value = 0.0238), however not across sessions (Pearson's correlation, p-value = 0.0728) (Figure 12). The correlation of rewarded trials of ChR2-expressing mice showed an increase in correlation within (Pearson's correlation, p-value = 0.0051 < 0.05) and across (Pearson's correlation, p-value = 0.0152) sessions (Figure 12). For both groups, the median correlation of the movements was organized into a heat map with black arrow representing within sessions and gray arrow representing across sessions (Figure 12). No significant difference in correlation of rewarded trials between wildtype and ChR2-expressing mice was shown. Results from both conditions were similar to normal learning data acquired from previous studies[11].

Furthermore, as data was being analyzed, we observed that ChR2-expressing mice were more active before the onset of the cue (data not shown). Therefore, we questioned if ChR2-expressing mice were more active only before the onset of the cue or throughout the whole session. Thus, number of lever active epics within the intertrial interval were analyzed for each session between the two groups throughout the 14 days of learning. Results indicated ChR2-expressing mice moved more during the ITI, no light stimulation period, than the control mice (Figure 13a.). The integrated number of

movements over all 14 sessions was also analyzed and ChR2-expressing mice showed, on average, a higher number of movements during the ITI (~35 movements) when compared to the wildtype mice (~25 movements) (Figure 13b).

In addition, images from labeled cells in the SI and M1 were compared between the two viruses used in these experiments. By visual observation, the density of labeled cells for both ChAT and ChR2 looked less in the ChR2-tdTomato-injected mice than in the ChR2-EYFP-injected mice (Figure 8 and 9). Thus, cells that were both positive for ChAT and ChR2-tdTomato within the SI were quantified to gain insight on how well the cells were infected with the virus. On average, only about 34% of ChAT-positive cells were infected with ChR2-tdTomato within the SI (Figure 14).

Lastly, immediate early genes were labeled to confirm the activation of cholinergic fibers expressing ChR2 in the motor cortex. Immediate early genes, such as Npas4, help us identify activated neurons[26]. Npas4 was labeled within the mouse motor cortex of trained mice injected with either ChR2-tdTomato or saline. In addition, a mouse in homecage that underwent no training or surgery was also labeled for Npas4 expression. No Npas4 expression was seen in the SI, but labeled cortical cells were seen in all three conditions (Figure 15). Labeled cortical cells need to be quantified to deduce if training and/or acetylcholine system upregulation lead to an increase in activated cortical cells.

Figures:

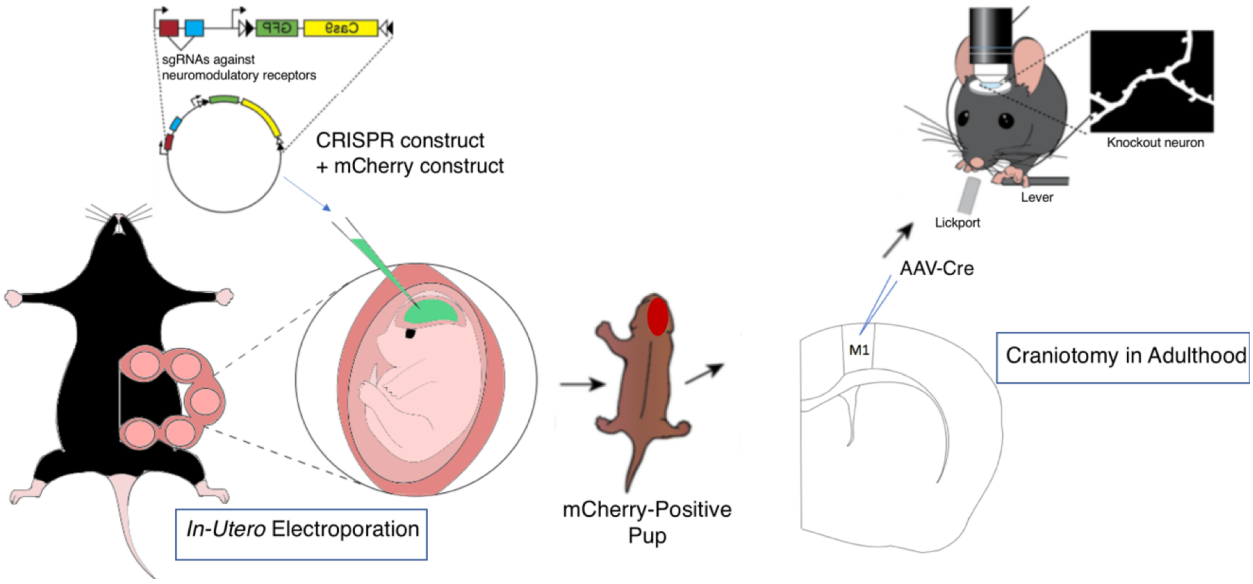

Figure 1: Series of techniques used for loss-of-function experiments. A CRISPR construct, designed to target deletion of a specific receptor type, and an mCherry construct are injected into timed embryonic brains within the left ventricle via *in utero* electroporation. Once born, pups are immediately checked for mCherry expression over their motor cortex to confirm the successful introduction of the CRISPR construct. After growth and maturation, the mice undergo craniotomies and viral injections of diluted AAV-Cre into L2/3 of M1. Introduction of Cre flipped the Cas9-GFP gene into the sense direction and initiate its expression, ultimately, leading to knockout of a specific receptor type within the cell. Afterwards, mice undergo a two-week training period of a lever-press task. During this time, targeted neurons for neuromodulatory receptor deletion was imaged.

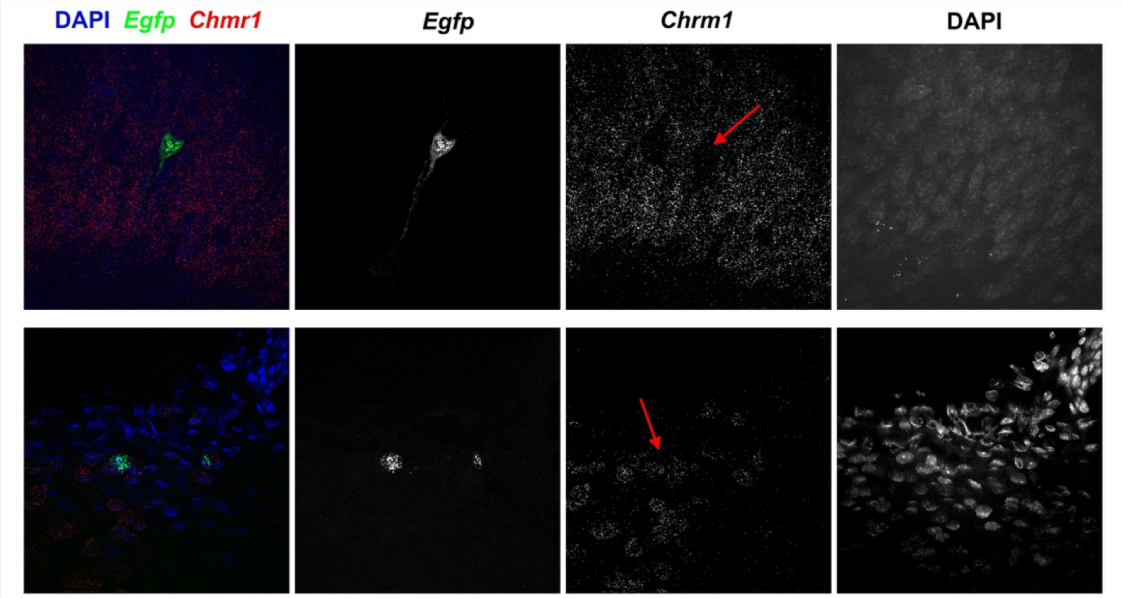

Figure 2: Successful CRISPR-based removal of targeted mRNA using RNAscope. Confocal images of the RNAscope procedure on cells targeting deletion of CHRM1 (cholinergic receptor M1) gene (gCHRM1-Cas9-EGFP) via CRISPR-based genome editing by using biolistics. The presence of EGFP mRNA signifies a cell transfected with a CRISPR construct designed to knock out the gene. Arrows indicate locations corresponding to a transfected/ EGFP-positive cell which lacks CHRM1 signal (red), suggesting successful removal of the CHRM1 gene. DAPI stains for all cell nuclei, EGFP labels mRNA within cell with CRISPR construct, and CHRM1 labels mRNA expressed from the gene. Data was acquired from Miguel Tillo, PhD (Bloodgood Lab).

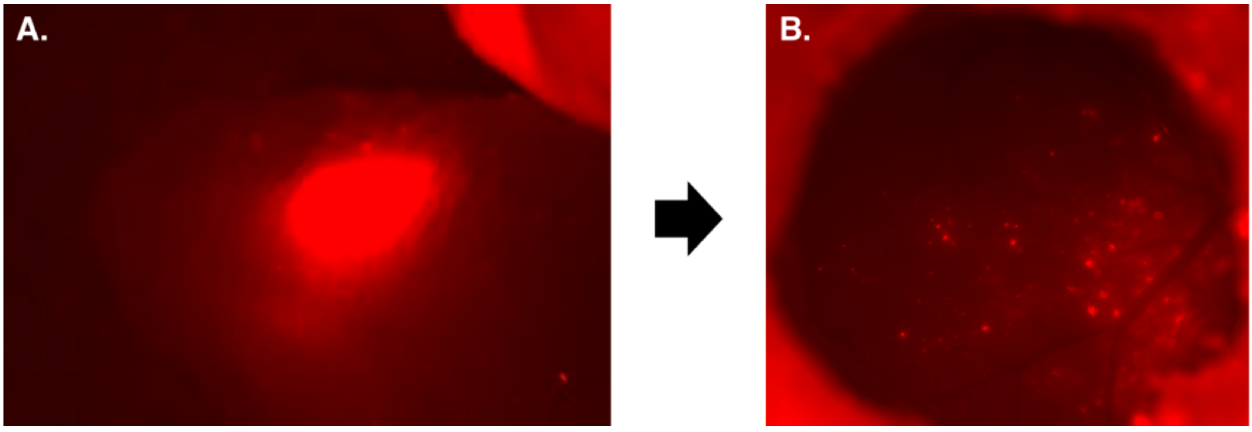

Figure 3: Successful delivery of CRISPR construct via IUE and survival from birth through adulthood. mCherry expression is visualized within the motor cortex (a) through the skin of mice at birth and (b) through the cranial window in adult mice. Successful delivery of constructs to a sparse population are confirmed as only a few cells are labeled red within M1 during adulthood. During craniotomies in adulthood, location of mCherry expression guides AAV-Cre injection.

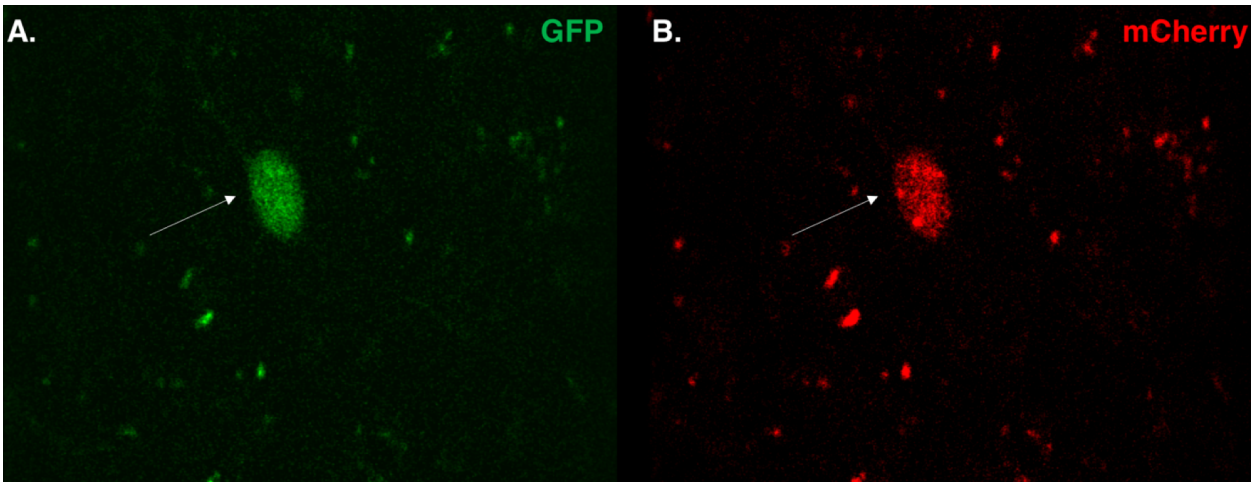

Figure 4: Successful Co-expression of GFP- and mCherry-positive cells *in vivo*. Arrow indicates a GFP-positive (a) and mCherry-positive (b) neuron in L2/3 of M1 in an alive, behaving mouse using two photon calcium imaging. GFP expression is too dim to follow neuronal morphological changes throughout time.

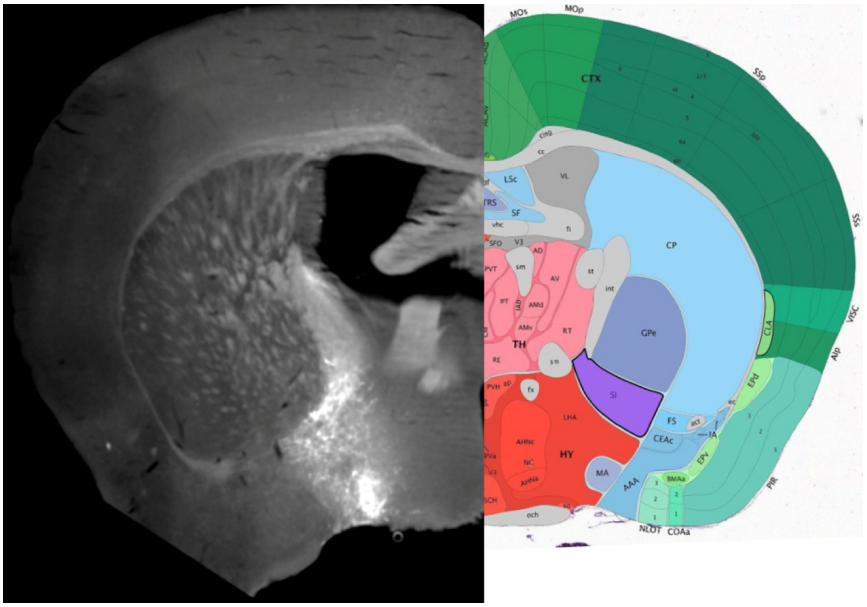

Figure 5: Confirmation of injection site (SI) through histology. Image of 60um coronal section of mouse brain stained against GFP 10 days post-injection of FLEX-ChR2-YFP in the ChAT-Cre mouse line. The right image is taken from the Allen Brain Atlas with the desired target area outlined in bold. By comparing the coronal brain slice obtained from our experiments to the Allen Brain Atlas, we can confirm that the ChAT-Cre mouse has appropriate expression of the injected CHR2-YFP within the SI.

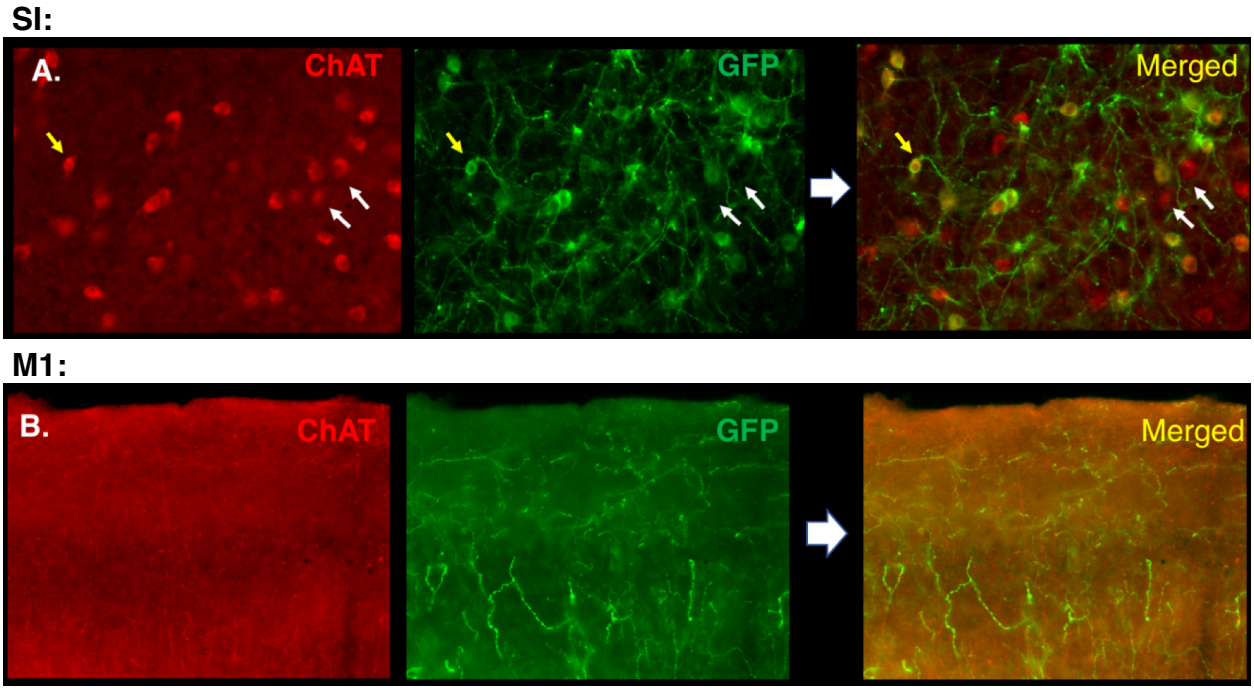

Figure 6: Co-labeled ChAT- and ChR2-EYFP-positive cells in SI and M1 Confirms Target Site. All images are from 40 um coronal sections of ChAT-Cre mice 10 days post-surgery. GFP was used to amplify expression of ChR2-EYFP. A. Yellow arrow indicates a neuron in the SI co-labeled with ChAT and ChR2-EYFP. White arrows indicate cholinergic cell bodies not infected with ChR2-EYFP. B. Confirms co-expression of ChAT and ChR2-EYFP in axons in the motor cortex indicating the presence of cholinergic axons projecting from the SI infected with ChR2-EYFP.

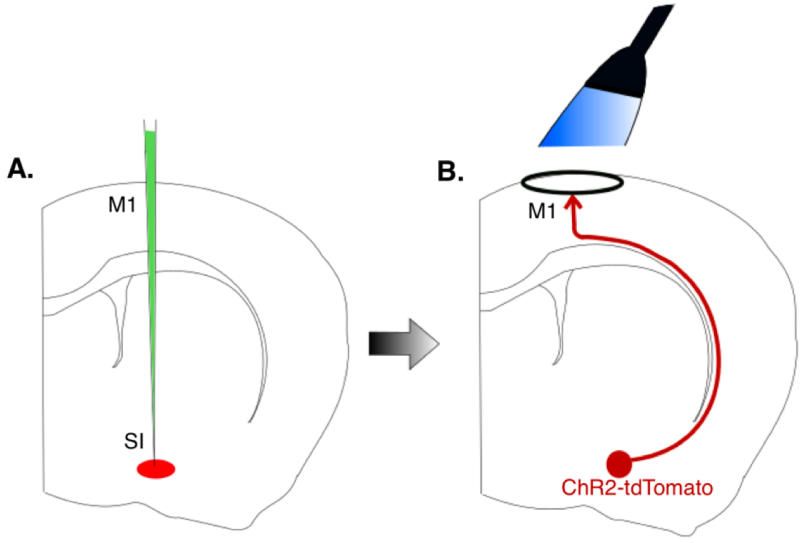

Figure 7: General procedure for gain-of-function experiments. A. Adult ChAT-Cre mice are injected with either ChR2-tdTomato or saline into the substantia innominata. B. After 3-4 weeks, blue light is shown over the cranial window during behavioral training and cholinergic fibers projecting from SI to M1 expressing ChR2-tdTomato are upregulated upon illumination.

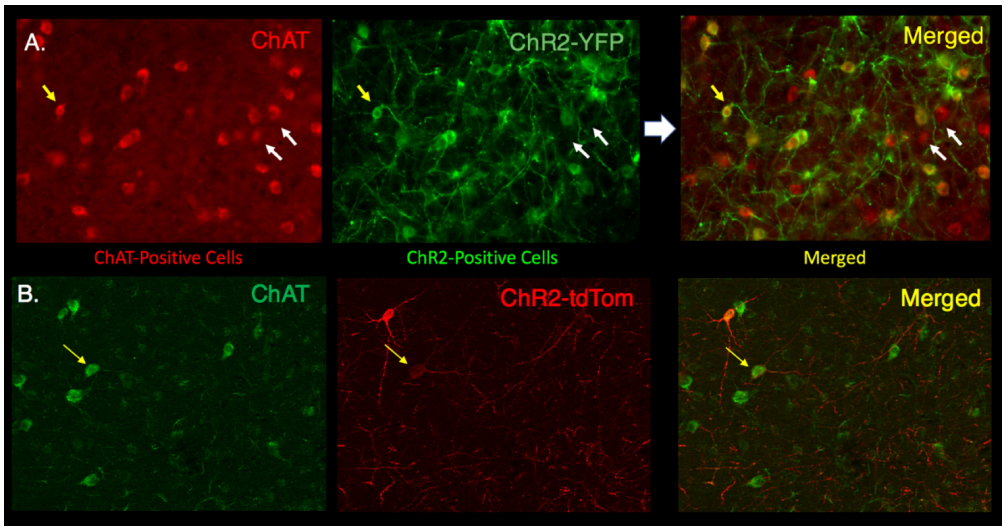

Figure 8: ChR2-EYFP vs ChR2-tdTomato-positive cells in SI. Images of 40um coronal sections of mouse brains expressing ChAT and ChR2. Images of (a) correspond to a mouse injected with ChR2-YFP and (b) corresponds to a mouse injected with ChR2-tdTomato. By visual observation, there seems to be a higher density of expressed ChR2-YFP cells than ChR2-tdTomato cell bodies in the SI. There is also more colocalization of the ChAT- and ChR2-positive cells in mouse (a) with the ChR2-YFP injection.

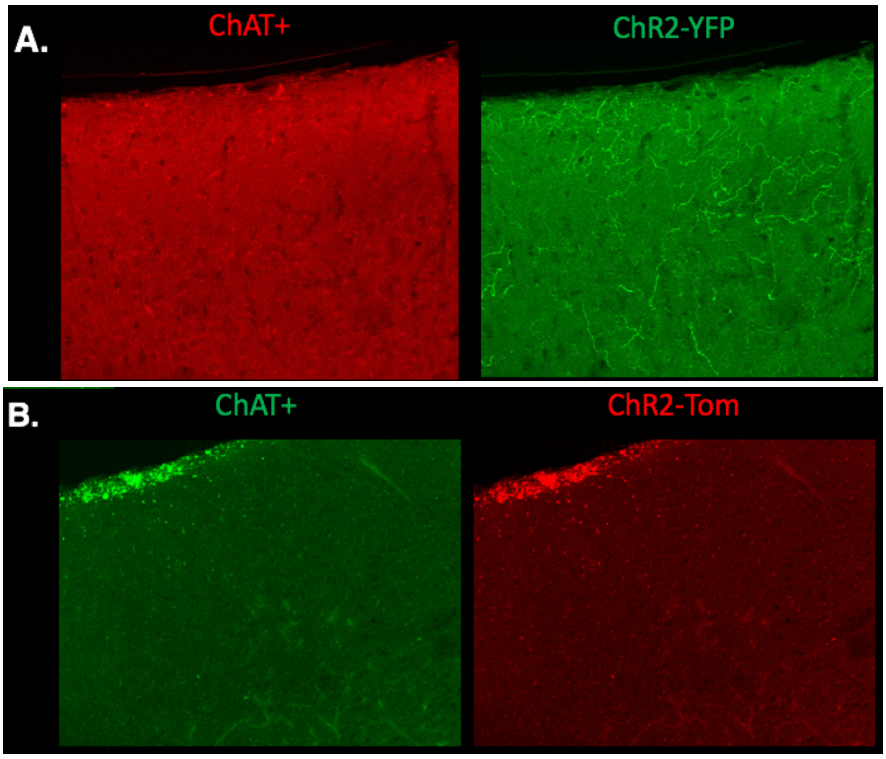

Figure 9: ChR2-EYFP vs ChR2-tdTomato-positive axons in M1. Images of M1 axon expression labeling ChAT and ChR2-positive conditions in 40um coronal sections of mouse brains. Images of (a) correspond to a mouse injected with ChR2-YFP and (b) corresponds to a mouse injected with ChR2-tdTomato. Axons are more apparent in the ChR2-YFP injected mice (a).

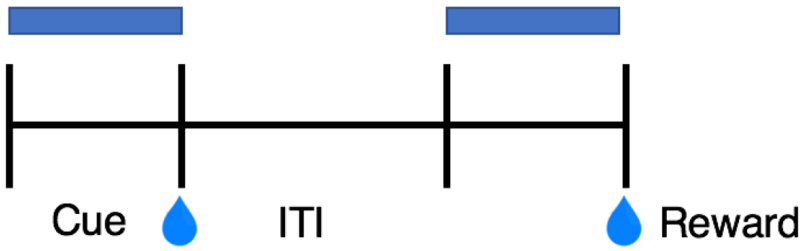

Figure 10: Task schematic. Behavioral Training consists of a cue period beginning with an auditory cue and illumination of blue light throughout the whole cue period. The cue period is terminated early if mouse receives water reward. If the mouse does not receive a water reward, then they hear white noise. Then, the inter-trial interval (ITI) follows with no light stimulation. Blue bars are temporal representations of blue light illumination over the animal's motor cortex.

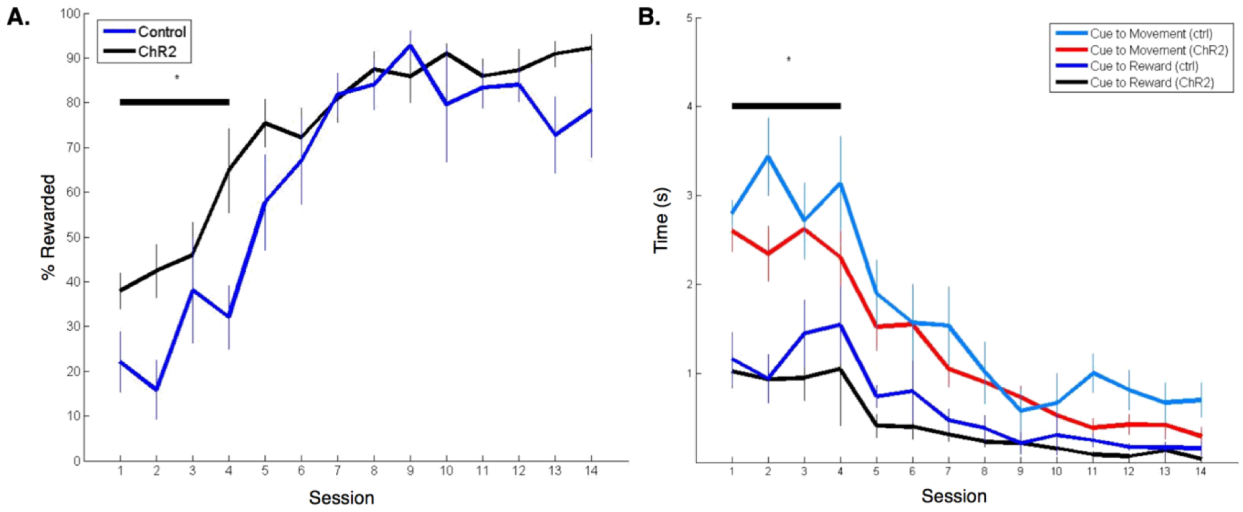

Figure 11: ChR2-expressing mice show higher reward rate (a) and faster reaction time during pre-learning stages (b). Black bar and asterisks indicate significant difference between the groups.

Control Mice (n=9)

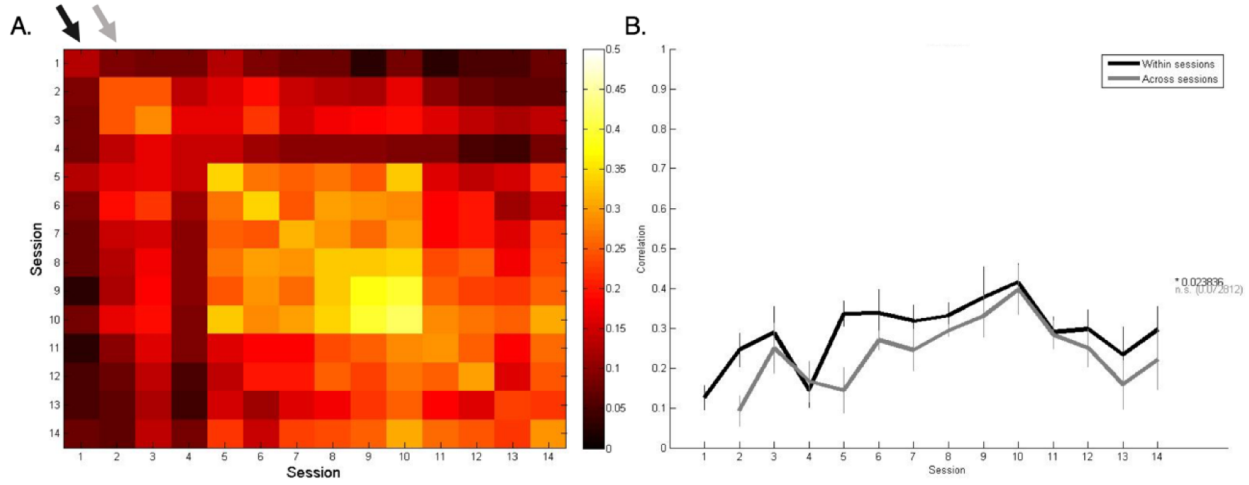

ChR2-expressing Mice (n=12)

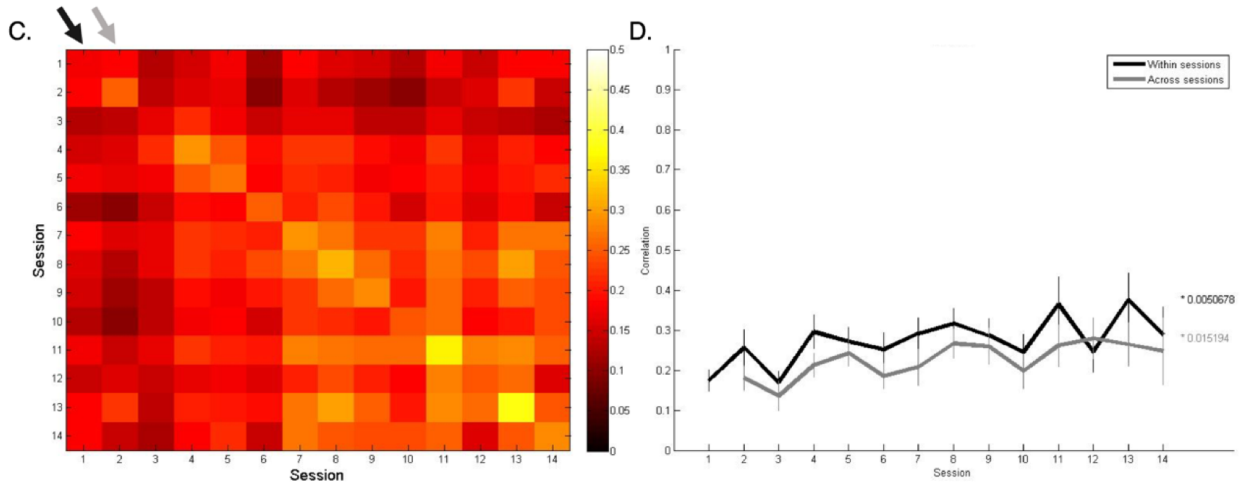

Figure 12: No significant difference in correlation of rewarded trials between control vs. ChR2-expressing mice. Data acquired from 9 control mice (a,b) and 12 ChR2-expresssing mice (c,d). Median pairwise correlation coefficients of rewarded movements on individual trials over 3 seconds, averaged across control animals (a) and ChR2-expressing mice (c). Pairwise movement correlation within and across sessions of control mice (b) and ChR2-expressing mice (d). Within sessions (black) and across sessions (gray) data from graph b corresponds to the respective colored arrows on top of the heat map in a. Similar distinction is seen in figure c and d. Results from both conditions are similar to normal learning data acquired from previous studies[11].

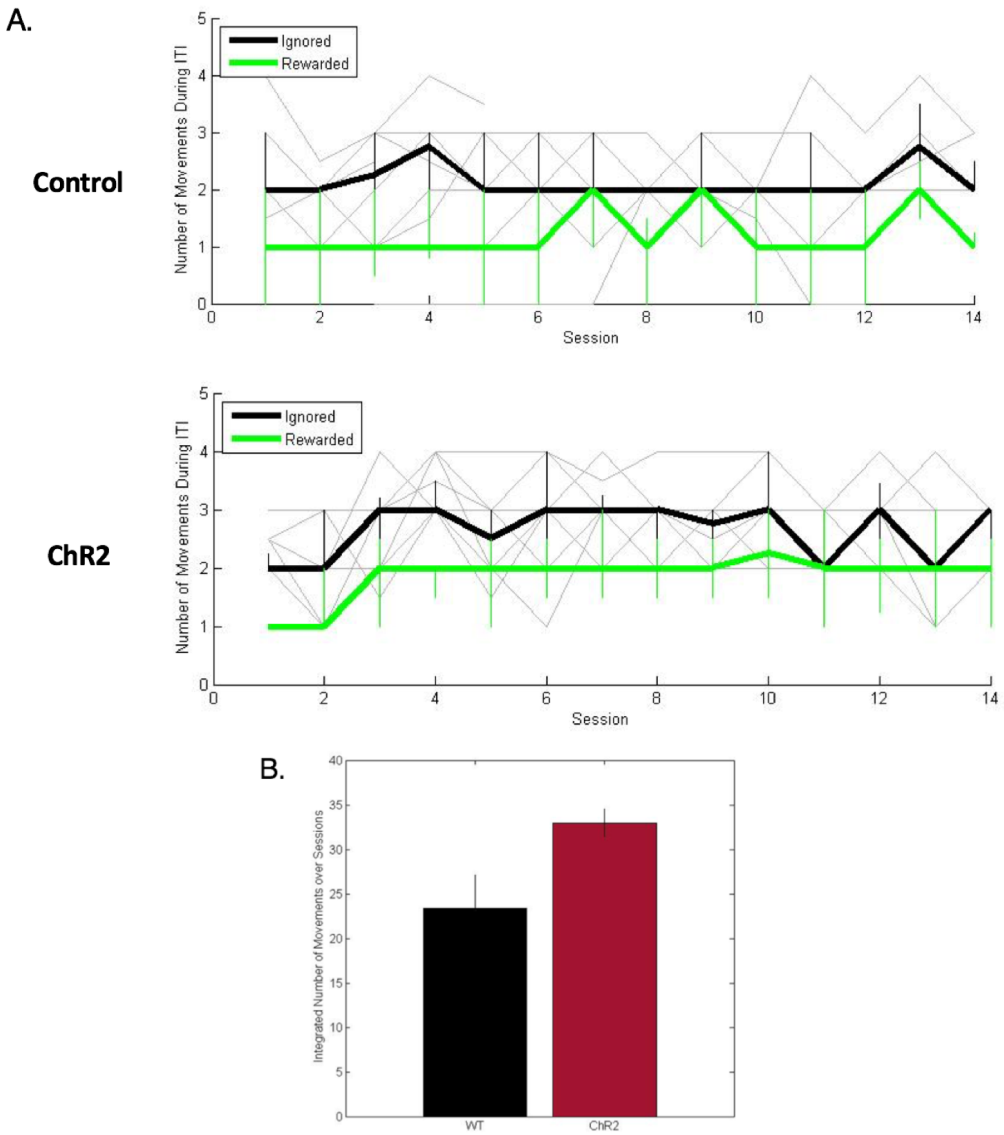

Figure 13. ChR2-expressing mice move more during ITI – no light stimulation period. (a) Number of movement during ITI represented number of lever active epics during the ITI. ChR2-expressing mice displayed a relatively constant increase by one in movement during ITI in both ignored and rewarded trials throughout the two weeks of learning. Ignored trials represent trials in which the mouse was moving before the onset of the cue. (b) The integral of the median was taken from the data acquired in a to display the integrated number of movements over sessions between the two conditions. ChR2-mice displayed a greater number of movements over sessions.

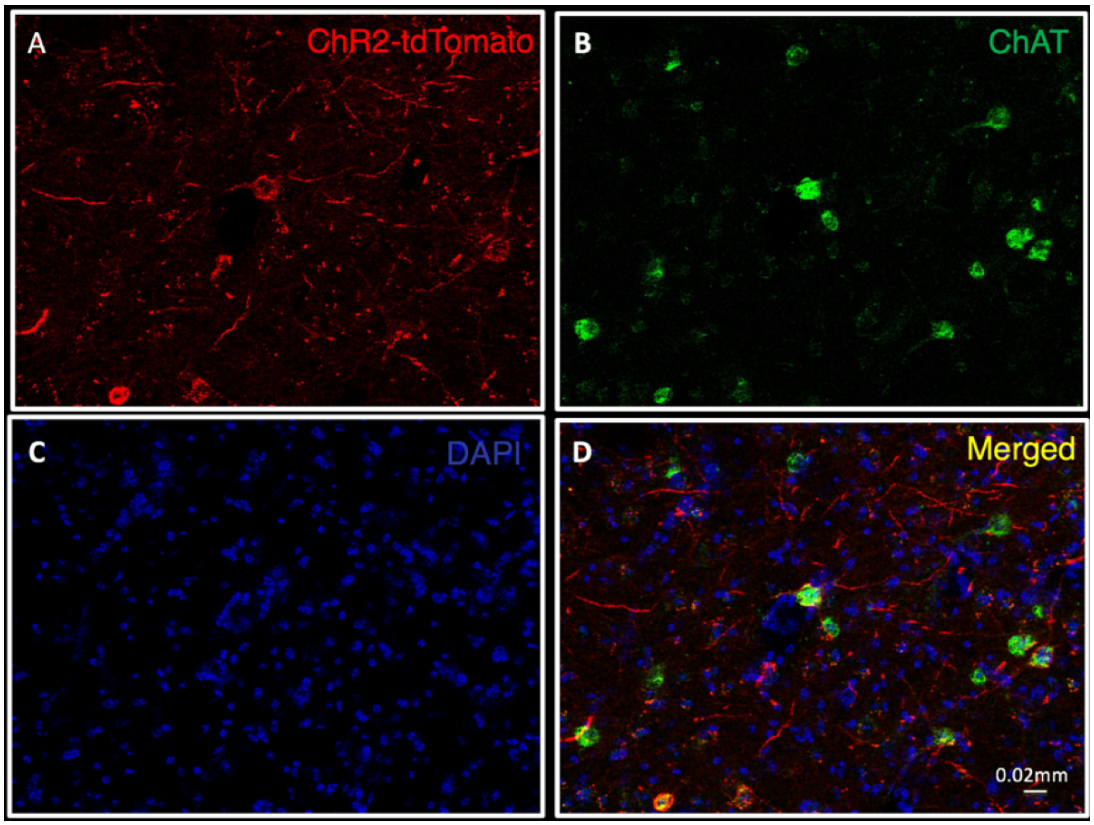

Figure 14: Quantification of infected cells with ChR2-tdTomato. Image of SI of a 40um coronal section of mouse brain with (a) endogenous expression of ChR2-tdTomato and stained against (b) GFP for ChAT expression and (c) DAPI for nuclei expression three weeks post-injection. An image overlapping all three fluoresce images is shown in (d). DAPI was used to help identify cells rather than artifacts in the quantification process. ChR2-tdTomato positive cells were counted manually from the image as were ChAT-positive cells within the SI. After this quantification method was applied from all the images of the SI from all the mice, we found that, on average, about 34% of ChAT-positive cells were infected with ChR2-tdTomato within the SI.

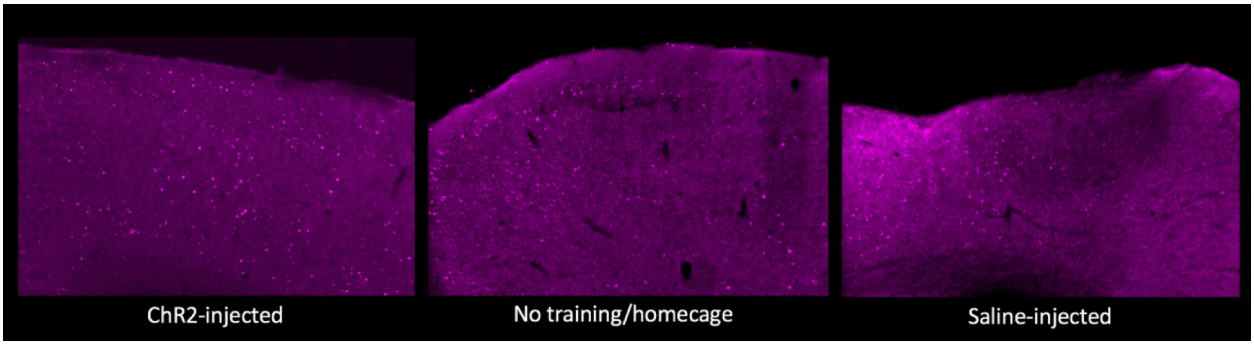

Figure 15. NPAS4 labeling. Images of M1 in 40um coronal sections of mouse brains stained against NPAS4. ChR2- and saline-injected mice were stained post-injection and post-training. The mouse in homecage did not undergo surgery or behavioral training.

Discussion:

To gain a mechanistic understanding of the role of neuromodulators in learning, we conducted loss- and gain-of-function experiments. Our loss-of-function experiments served a technical side to our project. We targeted the deletion of specific neuromodulatory receptors using CRISPR. Although the experimental portion of this project was not able to be fully carried out during the allotted time due to unforeseen obstacles, we were still able to show success in performing and confirming the validity of our cutting-edge techniques. Firstly, the CRISPR constructs were validated to perform successful knock-out of a specific neuromodulatory receptor type *in vitro* using RNAscope. These results allowed us to introduce these constructs *in vivo.* Next, we became more successful at introducing these constructs into embryonic mice brains via *in utero* electroporation as confirmed by mCherry expression in M1 of electroporated pups and in their adulthood. We were also successful in introducing AAV-Cre to the same population of cells with mCherry expression to allow for successful inversion of the Cas9-GFP gene and expression as denoted by both the presence of GFP expression and co-labeling of GFP and mCherry expression within the same population of cells. We also confirmed our surgeries targeted a sparse population of L2/3 neurons in M1. However, we were unable to continue the behavioral and imaging experiments since the GFP expression *in vivo* was too dim. Unfortunately, the dim expression hindered our ability to measure the resulting change in plasticity in neurons with neuromodulatory receptor knock-out.

Due to this obstacle, we investigated for other methods to overcome the dimness in GFP expression *in vivo*. Currently, we are continuing the experiments in the lab using a flippase approach. Briefly, in this approach, the GFP gene is no longer expressed in the CRISPR construct introduced via IUE, but rather within the Cre-dependent virus introduced during the craniotomy. This allows for GFP expression to be less dependent on the success of the IUE procedure and more on the titer of the virus used during craniotomies. Therefore, genetically modified cells are denoted by green fluorescence indicating that they are both labeled by the IUE plasmid and infected by Cre.

Our loss-of-function experiments showed that the surgeries and methodologies used were successful. So, our experiments will continue using the same methodologies with the flippase approach to investigate the mechanistic role of neuromodulators on learning.

On the other hand, for our gain-of-function experiments, our preliminary results supported our hypothesis to some degree. Our hypothesis was that since acetylcholine is associated with attention, then we would see an affect during the early stages of learning and an acceleration of the learned behavior. Although our sample size was small and different between the two groups (control group, n = 9; ChR2-injected group, n = 12), we still obtained some differences between the two groups. However, for better results, we would need a larger sample size for both groups.

From our preliminary results, ChR2-injected mice showed a difference in the early stages of learning such that they had a greater percent rewarded trials and lower cue-to-reward times. However, we saw no difference between the two groups in

correlation. Surprisingly, we found that ChR2-injected mice moved more before the onset of the cue during the later stages of learning. These findings piqued our interest to investigate the movements during different time intervals. This led us to find that ChR2-injected mice had a greater number of movements during the ITI. Due to the type of control group we utilized, the difference in movements between the two groups was not due to the light stimulation itself, but rather may be due to the introduction of ChR2.

Therefore, besides having a small population size that may be preventing us from seeing a difference in correlation between the two groups, there are also two possible explanations for our results. Firstly, there may have been insufficient infection and activation of ChR2. On average, about 34% of ChAT cells were infected with ChR2-tdTomato in the SI. Also, by observation, we visualized less dense and dim expression when using ChR2-tdTomato compared to ChR2-EYFP (Figure 8 and 9). Thus, our next step will be to confirm this difference by quantifying the average density of labeled ChR2-EYFP cells within the SI and compare it to ChR2-tdTomato injected mice. We will also repeat the upregulation experiments with ChR2-EYFP and compare the behavioral results. ChR2-EYFP has a brighter fluorescence that will help us visually quantify the density of infection. This follow-up experiment could indicate if we are not sufficiently infecting the cholinergic neurons in the SI and if ChR2-tdTomato was not the best virus to use for our experiments.

A second possible explanation to our results is that the acetylcholine system within the motor cortex may already be saturated. If our behavioral data does not in fact show a difference in correlation in ChR2-injected mice due to the hyperactivation of the

ACh system, then this does not mean that ACh is not involved in learning. There is the possibility that the ACh system is simply saturated. To test for saturation, we will conduct follow-up experiments and inject halorhodopsin using the same approach for reversible silencing of the neurons. Since we did not see any changes in learning with optical excitation in terms of correlation, then if we do see behavioral effects with the downregulation of the NM system with the introduction of halorhodopsin, then this would support that the acetylcholine system is simply saturated. If we find that the acetylcholine system is saturated, then this could also potentially call cognitive enhancers into question because these may not be exerting their effects under saturating conditions, leading to the placebo effect[26].

Furthermore, we tried to visualize activated cells by staining for Npas4, an indicator of neural activity (Figure 15)[25]. In three different conditions, we were able to activate cortical cells; however, we were unable to visualize activated ChAT cells in the SI. This could be due many possibilities, such as ChAT cells not expressing NPAS4 or the ChAT neuronal population is not being activated. From our results, we confirmed that for Npas4 staining, the antibody works. Next, we will quantify and compare the density of labeling in untrained and trained mice, and then see if there are any differences in cortical neuronal activation when the cholinergic system is upregulated within the motor cortex. Simultaneously, we will search for a better marker for cholinergic cells to confirm their activation within our experiments. All in all, by gaining a mechanistic understanding of the neuromodulatory role on learning, we can study the effects of neuromodulators on learning in both normal and diseased brains.

Methods:

Animals.

All procedures were in accordance with protocols approved by the University of California, San Diego Institutional Animal Care and Use Committee and guidelines of the National Institute of Health. Swiss Webster (CFW) mice were acquired from Charles River Laboratory for the loss-of-function experiments and knock-in recombinant mice strain B6;129S6-Chat$^{tn2(cre)Lowl}$/J acquired from The Jackson Laboratory. All surgeries and experiments were carried out in adult mice (6 weeks or older). All mice were housed in disposable plastic cages with standard bedding in a room on a reversed light cycle (12 h/12 h), before surgery and after recovery from surgery. Most behavioral experiments were performed at approximately the same time each day for each mouse. All animals were water-restricted before training and received ~1-2mL of water a day. Experiments were conducted mostly during the night cycle.

Loss-of-function Experiments

***In Utero* Electroporation (IUE).**

Unilateral electroporation was performed to target the right neocortical L2/3 neurons. The surgical procedure was followed as described[12,27]. Pregnant female mice were prepared for surgery on E15.5 to target neocortical M1 L2/3 neurons. The mice were anesthetized with isoflurane and injected with buprenorphine (pain reliever, 0.1 mg/kg) and Baytril (antibiotic, 10 mg/kg) subcutaneously. The embryonic brains were injected with DNA (2-3ug/uL) with 10% FastGreen dye into the right lateral ventricle. The plasmids were directed to the motor cortex to label excitatory neurons

by positioning the positive electrode over the injection site. Then, five electric pulses of 50ms at 40-50V with 1s intervals were delivered using a triple-electrode probe square wave electroporation generator (Harvard Apparatus) for DNA to migrate into the targeted excitatory neurons. After surgery, pups continued normal development until born. Once born, the pups were checked under a Zeiss AxioZoom.V16 wide-field microscope. Successful transfection of live pups was confirmed by red fluorescent on the surface of the right motor cortex. The mice were matured until adulthood for later surgery.

Craniotomies.

Male and female adult Swiss Webster (CFW) mice acquired from Charles River Laboratory were anesthetized with isoflurane and injected with buprenorphine (pain reliever, 0.1 mg/kg), Baytril (antibiotic, 10 mg/kg) and dexamethasone (anti-inflammatory, 2 mg/kg) subcutaneously. Their eyes were covered with Vaseline to prevent corneal drying during the surgical procedure. The animal's scalp was disinfected with ethanol and betadine. The animal's skull was exposed, the surface disinfected with ethanol, and a three-prong custom head plate was glued and cemented to the skull. A craniotomy was performed at 300 μm anterior and 1,500 μm lateral from bregma over the right caudal forelimb area in M1[12,28-29].

Viral injections.

Once the skull was peeled, the exposed brain was viewed under a Zeiss AxioZoom.V16 wide-field microscope to check for presence and location of red

fluorescence to guide viral injections. AAV2/1-CMV-PI-Cre (1:5,000; UPenn Vector Core) diluted with saline was injected at 4-5 locations with volume of 20-30 nL at each site 500 μm apart and 250 μm depth to target layer 2/3 cells in M1. After viral injections, a glass window was placed over M1 and secured with Vetbond and dental acrylic. After surgery, mice remained on the heating pad for 30 minutes until recovered. No motor impairments were observed by the mice after surgery. Mice continued to recover for two weeks until training and imaging.

Behavior.

Animals were trained in a simple lever-press task as previously described[11-12]. Healthy, recovered mice were water-restricted (1-2mL per day) after three days from surgery for 2 weeks until training. Mice were water-restricted to motivate their performance in the task, and thus were trained daily for 14 days with simultaneous two-photon imaging applied (1 session per day; ~30min each session). Mice placed their left forelimb on a movable lever which was built using a piezoelectric flexible force transducer (LCL-113G, Omega Engineering) attached to a 1/16-mm-thick brass rod. The voltage from the force transducer was linearly proportional to the lever position. These voltage readings were continuously recorded using a data acquisition device (LabJack) and software (Ephus, MATLAB, Mathworks; LabVIEW, National Instruments). Software (Dispatcher, Z. Mainen and C. Brody) running on MATLAB controlled the behavioral setup and communicated with a real-time system (RTLinux). The cue onset began with 6-kHz tone and continued until the mouse pressed the lever and was rewarded with water (~8 uL per trial) and heard a 500-ms, 12-kHz tone, followed by an

inter-trial interval. The crossing of two thresholds (~2mm and ~4mm below the resting position) within 200 ms defined the lever-press. This ensured that mice were only rewarded when they pressed the lever in a more defined manner within the time frame rather than continuously holding the lever down or gradually pressing the lever beyond the thresholds over longer periods of time. When mice failed to successfully press the lever during the cue period, a loud white noise was triggered and began the onset of the inter-trial interval. Each session lasted 20-30 min and 100-200 trials or until the mouse stopped performing.

Imaging.

During behavioral sessions, imaging was performed on awake, behaving animals using a two-photon microscope (B-scope, Thorlabs) running Scanimage using a 16X objective (Nikon) with excitation at 925nm (Ti-Sa laser, Newport). For structural imaging of neurons, z-stack images were obtained at 20 frames per plane, 80-120 planes per animal with a *z*-axis step size of 1-µm. Lateral motion correction is performed post hoc for each image plane of 20 frames by full-frame cross-correlation image alignment (Turboreg plug-in in ImageJ). The reference image was set as the average of the 5 most consistent consecutive frames. Next, the 20 frames from the image plane were averaged, and various image planes were aligned using recursive alignment of stacks of images using Stackreg (ImageJ).

Perfusion and Histology.

Mice were anesthetized and transcardially perfused with ice-cold 0.1M PBS (pH 7.4), then by perfusion with ice-cold 4% paraformaldehyde (PFA) solution. The animal's brain was isolated and stored overnight at 4 °C in 4% PFA, then cryoprotected in 30% sucrose solution for at least 24 hours at 4 °C.

Coronal sections were obtained at 40-60µm using the microtome Thermo Scientific Micro HM 430. The free-floating brain sections were collected in PBS and stored at 4 °C.

For immunostaining, the sections were incubated in goat blocking buffer consisting of 10% normal goat serum, 1% BSA and 0.3% Triton 100-X in 1xPBS for 1 hour at room temperature with gentle agitation. The slices were then incubated overnight at 4 °C with gentle agitation with primary antibody solution (chicken anti-GFP 1:1000, GFP-1020, Aves Labs, Inc.; rabbit anti-mCherry 1:300, ab167453, Abcam) diluted in 0.003% normal goat serum and 1xPBS. Next, the slices were washed with PBS for 10 minutes at room temperature with gentle agitation, repeated three times. Then, the slices were incubated in secondary antibody solution (AlexaFluor488, goat anti-chicken 1:1000, Invitrogen; AlexFluor594, goat anti-rabbit 1:1000, Life Technologies) diluted in PBS and incubated for 2 hours at room temperature with gentle agitation. Next, the slices were washed with PBS for 10 minutes at room temperature with gentle agitation, repeated three times. The slices were mounted on a glass slide, and cover-slipped. Slides were stored in 4°C and protected from light until viewing under the microscope.

Images of brain coronal sections were taken with either a Zeiss AxioZoom.V16 wide-field microscope or Zeiss Imager M2 with the Apotome.2 attachment, controlled with AxioVision 4.8 software. Color levels were post-processed using ImageJ.

Gain-of-Function Experiments

Stereotaxic surgery and viral injection.

Male and female adult mice were anesthetized with isoflurane and injected with buprenorphine (pain reliever, 0.1 mg/kg), Baytril (antibiotic, 10 mg/kg) and dexamethasone (anti-inflammatory, 2 mg/kg) subcutaneously. The mice were then placed in a stereotaxic frame and their eyes were covered with Vaseline to prevent corneal drying during the surgical procedure. The animal's scalp was shaved and disinfected with ethanol and betadine. Next, the animal's skull was exposed by removing the skin above the skull and separating the muscle tissue. The surface of the skull was disinfected with ethanol and hydrogen peroxide. Using the micromanipulator and the probe of the stereotaxic instrument, the mouse's brain was leveled within a +/- 20nm range. Bregma, the point where the sagittal suture intersects with the coronal suture, served as the origin of the coordinates at (0,0) for all the mice. Next, the fascia was removed from the animal's skull and a steel head bar was implanted onto the skull. A craniotomy was performed at 300 μm anterior and 1,500 μm lateral from bregma over the right caudal forelimb area in M1 and blind injections were performed with either 200-300nL of saline or AAV1.CAGGS.flex.ChR2-tdTomato.WPRE.SV40 (UPenn Vector Core) into the substantia innominata, 4,400 μm from the brain's surface, 1,800 μm

lateral, and 300 μm anterior from bregma, An optical glass window was placed over the craniotomy and fixed in place with Vetbond Tissue Adhesive and dental cement. After surgery, mice remained on the heating pad for 30 minutes until they recovered. No motor impairments were observed by the mice after surgery.

Behavior and Optical Stimulation.

Mice expressing Cre-recombinase downstream the ChAT promoter were blindly injected with either saline or virus encoding ChR2-tdTomato into the substantia innominata. Training began 3-4 weeks after surgery for optimal expression of ChR2[25]. Mice were water-restricted at 1-2 mL of water per day, then trained daily to perform a simple lever-press task for 14 days, 1 session per day. Behavior experiments were performed as noted in the loss-of-function methods. During behavior, blue light pulses were delivered from an LED (~3mW,~ 0.5mm diameter, Doric Lenses) onto the center of the cranial window over M1 throughout the entire cue period of 10 seconds for each trial of each session (~30 min per session). The inter-trial interval lasted 8-12 sec.

Perfusion and Histology.

Mice were anesthetized and transcardially perfused with ice-cold 0.1M PBS (pH 7.4), then by perfusion with ice-cold 4% paraformaldehyde (PFA) solution. The animal's brain was isolated and stored overnight at 4 °C in 4% PFA, then cryoprotected in 30% sucrose solution for at least 24 hours at 4 °C.

Coronal sections were obtained from tissue at 40-50µm coronal slices using the microtome Thermo Scientific Micro HM 430. The free-floating brain sections were collected in PBS and stored at 4 °C.

Immunostaining (SE0012-21):

For ChAT and ChR2 staining, the slices were incubated in donkey blocking buffer (10% normal donkey serum, 1% BSA, 0.3% Triton 100-X) in 1xPBS for 2 hours at room temperature with gentle agitation. The slices were then incubated with primary antibody solution (goat anti-ChAT 1:200; rabbit anti-mCherry 1:300) diluted in donkey blocking buffer overnight at 4 °C with gentle agitation. Next, the slices were washed with PBS for 10 minutes at room temperature with gentle shaking, repeated three times. Then, the slices were incubated with secondary antibody solution (donkey anti-goat 488 1:1000; donkey anti-rabbit 594 1:1000) diluted in 1x PBS for 2 hours at room temperature with gentle agitation. The slices were washed again three times with 1xPBS for 10 minutes each at room temperature with gentle shaking. The sections were mounted on a glass slide, cover-slipped, and edges sealed with clear nail polish. Slides were stored in 4°C and protected from light until viewing under the microscope.

Immunostaining (SE0022-35):

For ChAT and Npas4 staining, the tissues were incubated in donkey blocking buffer (10% normal donkey serum, 1% BSA, 0.3% Triton 100-X) in 1xPBS at 4°C overnight with gentle agitation. Then, the slices were incubated with primary

antibodies (goat anti-ChAT 1:200, ab144p, Millipore Sigma; rabbit anti-Npas4 1:2000, Bloodgood Lab) diluted in an antibody buffer consisting of 0.25% Triton X-100, 10% donkey serum, and PBS. Sections were incubated over two nights at 4°C with gentle agitation. Next, the slices were washed with 1xPBS for 10 minutes with gentle agitation at 4°C, repeated three times. After the third wash, PBS was removed and replaced with the antibody buffer with diluted secondary antibodies (AlexaFluor488, donkey anti-goat 1:1000, Invitrogen; AlexaFluor647, donkey anti-rabbit 1:1000, Abcam). The sections were incubated overnight at 4°C with gentle agitation. Next, the tissues were washed with 1xPBS again three times for 10 minutes each. The sections were mounted on a glass slide, stained with DAPI, cover-slipped, and edges sealed with clear nail polish. Slides were stored in 4°C and protected from light until viewing under the microscope.

Images of brain coronal sections were taken with a Zeiss Imager M2 with the Apotome.2 attachment, controlled with AxioVision 4.8 software. Color levels were post-processed using ImageJ.

Quantification of Fluorescence.

Images of SI and M1 were taken from 40-50um coronal sections three weeks post-injection. All GFP-labeled cell bodies in the SI and axons in M1were manually counted as ChAT-positive cells. Then, all ChAT-tdTomato cell bodies and axons were manually counted and compared. As the labeled cells were quantified, merged fluorescent images of each mouse brain were also analyzed. M1 quantification was

challenging since labeled M1 axons were either too dim or invisible. Thus, images were separated as either labeled ChR2-tdTomato-positive axons versus labeled axons not visually present. To determine the average percent of ChAT cells infected with ChR2 in the SI, we took the number of ChR2-tdTomato-positive cells and divided by number of ChAT-positive cells present in the image. We then averaged all these values from the images obtained from all ChR2-tdTomato-injected mice.

Movement Analysis.

Movement analysis was as described previously[11]. Briefly, lever displacement traces allowed us to recognize movement bouts. Then, the lever's velocity was determined such that movement was identified past a velocity threshold. Lever threshold was also identified to distinguish more stereotyped movements for when the lever displacement went below this threshold. Trials in which animals were moving the lever 100ms before the onset of the cue were excluded in the trials-based analyses. Movement analysis was not only restricted to movements that led to reward. All movements were analyzed by each mouse, including movements that did not lead to reward, movements made during the onset of the cue, and movements during the intertrial interval.

Pairwise Activity Correlation Analysis.

Pairwise activity correlation analysis was used as described previously[11-12]. Pearson's correlation coefficient was used during the analysis. Movements were

correlated to the learned movement, pairs of movements within sessions or across sessions were segregated with a maximum correlation with the learned movements.

Statistics.

When data may not fit a normal distribution, non-parametric tests were used. Control condition had a sample size of 9 and the ChR2-expressing mice had a sample size of 12. Individual trials were excluded when there were any confounding factors to the mouse's behavioral performance (e.g. lever press was broken or no water reward received in response to rewarded trials). Experiments were double-blinded.

References:

1. Montague PR, Dayan P, Sejnowski TJ. “A framework for mesecephalic dopamine systems based on predictive Hebbian learning.” *J. Neurosci,* 1996, 16: 1936-1947.

2. Parasuraman R, Greenwood PM, Kumar R, Fossella J. “Beyond heritability: neurotransmitter genes differentially modulate visuospatial attention and working memory.” *Psychol. Sci,* 2005, 16: 200-7.

3. Kety SS. “The biogenic amines in the central nervous system: Their possible roles in arousal, emotion, and learning.” *Neurosci. Second Study Progr,* 1970, 324–335.

4. Klinkenberg I, Sambeth A, Blokland A. “Acetylcholine and attention.” *Science Direct,* 2011, 221:430-442.

5. Molina-Luna K, Pekanovic A, Rohrich S, Hertler B, Schubring-Giese M, Rioult-Pedotti MS, Luft AR. “Dopamine in Motor Cortex is Necessary for Skill Learning and Synaptic Plasticity.” *PLoS One,* 2009, 17:4(9).

6. Conner JM, Culberson A, Packowski C, Chiba AA, Tuszynski MH. “Lesions of the basal forebrain cholinergic system impair task acquisition and abolish cortical plasticity associated with motor skill learning.” Neuron, 2003, 38: 819-829.

7. Carey MR, Regehr WG. “Noradrenergic control of associative synaptic plasticity by selective modulation of instructive signals.” *Neuron,* 2009, 62(1):112-22.

8. Izumi Y, Zorumski CF. “Norepinephrine promotes long-term potentiation in the adult rat hippocampus in vitro.” *Synapse*, 1999, 31(3):196-202.

9. Giessel AJ, Sabatini BL. “M1 Muscarinic Receptors Boost Synaptic Potentials and Calcium Influx in Dendritic Spines by Inhibiting Postsynaptic SK Channels.” *Neuron,* 2010,68: 936-947.

10. Dennis SH, Pasqui F, Colvin EM, Sanger H, Mogg AJ, Felder CC, Broad LM, Fitzjohn SM, Isaac JT, Mellor JR. “Activation of muscarinic M1 acetylcholine receptors induces long-term potentiation in the hippocampus.” *Oxford University Press,* 2016, 26: 414-426.

11. Peters AJ, Chen SX, Komiyama T. “Emergence of reproducible spatiotemporal activity during motor learning.” *Nature,* 2014, 510(7504):263-7.

12. Chen SX, Kim AN, Peters AJ, Komiyama T. “Subtype-specific plasticity of inhibitory circuits in motor cortex during motor learning.” *Nat. Neurosci,* 2015, 18:1109-115.

13. Doench JG, Fusi N, Sullender M, Hegde M, Vaimberg EW, Donovan KF, Smith I, Tothova Z, Wilen C, Orchard R, Virgin HW, Listgarten J, Root DE. “Optimized sgRNA design to maximize activity and minimize off-target Effects of CRISPR-Cas9.” *Nat. Biotechnol,* 2016, 34:1-12.

14. Holtmaat A, Keck TM, Knott G, Lee WC. “Long-term, high-resolution imaging in the mouse neocortex through a chronic cranial window.” *Nature protocols*, 2009, 4.

15. Lin D, Boyle MP, Dollar P, Lee H, Lein ES, Perona P, Anderson DJ. “Functional identification of an aggression locus in the mouse hypothalamus.” *Nature*, 2011, 470:221-226.

16. Wu H, Williams J, Nathans J. “Complete morphologies of basal forebrain cholinergic neurons in the mouse.” *eLife,* 2014, 3:e02444.

17. Rye DB, Wainer BH, Mesulam MM, Mufson EJ, Saper CB. “Cortical projections arising from the basal forebrain: a study of cholinergic and non- cholinergic components employing combined retrograde tracing and immuno- histochemical localization of choline acetyltransferase.” *Neuroscience*, 1984, 13:627-643.

18. Mesulam MM, Hersh LB, Mash DC, Geula C. “Differential cholinergic innervation within functional subdivisions of the human cerebral cortex acetyltransferase study.” *Journal of Comparative Neurology*, 1992, 318(3): 316-328.

19. McGaughy J, Kaiser T, Sarter M. “Behavioral vigilance following infusions of 192 IgG-saporin into the basal forebrain: Selectivity of the behavioral impairment and relation to cortical AChE-positive fiber density.” *Behavioral Neuroscience,* 1996, 110(2):247-265.

20. Sarter M, Martinez V, Kozak R, Parikh V. “Prefrontal acetylcholine release controls cue detection on multiple timescales.” *Neuron,* 2007, 56:141-154.

21. Young JW, Finlayson K, Spratt C, Marston HM, Crawford N, Kelly JS, Sharkey J. “Nicotine improves sustained attention in mice: evidence for involvement of the α7 nicotinic acetylcholine receptor.” *Neuropsychopharmacology,* 2004, 29:891-900.

22. Borrell V, Yoshimura Y, Callaway EM. “Targeted gene delivery to telencephalic inhibitory neurons by directional in utero electroporation.” *J. Neuroscience Methods,* 2005, 143:151-158.

23. Allen Institute for Brain Science. Mouse Brain. *Allen Brain Atlas* (2018).

24. Kalmbach A, Hedrick T, Waters J. “Selective optogenetic stimulation of cholinergic axons in neocortex.” *J Neurophysiology,* 2012, 7:2008-19.

25. Sun X, Lin Y. “Npas4: Linking Neuronal Activity to Memory.” *Trends Neuroscience,* 2016, 39(4):264-275.

26. Warburton, DM. “Nicotine as a cognitive enhancer.” *Prog Neuropsychopharmacol Biol Psychiatry,* 1992, 16(2):181-91.

27. Saito T, Nakatsuji N. “Efficient gene transfer into the embryonic mouse brain using in vivo electroporation.*” Dev Biol,* 2001, 240:237-246.

28. Kato HK, Chu MW, Komiyama T. “Dynamic Sensory Representations in the Olfactory Bulb: Modulation by Wakefulness and Experience.” *Neuron*, 2012, 76(5):962-975.

29. Komiyama T, Sato TR, O’Connor DH, Zhang TX, Huber D, Hooks BM, Gabitto M, Svoboda K. “Learning-related fine-scale specificity imaged in motor cortex circuits of behaving mice.” *Nature,* 2010, 464(7292):1182-6.